Grain Growth Kinetics of A_nB_n Star Block Copolymers in Supercritical Carbon Dioxide

Xiaochuan Hu, Samuel P. Gido,* and Thomas P. Russell*

Polymer Science and Engineering Department, University of Massachusetts, Amherst, Massachusetts 01003

Hermis Iatrou and Nikos Hadjichristidis

Department of Chemistry, University of Athens, Panepistimiopolis Zografou 15771, Athens, Greece

Ferass M. Abuzaina and Bruce A. Garetz

Department of Chemical and Biological Sciences and Engineering, Polytechnic University, Brooklyn, New York 11201

Received October 29, 2004; Revised Manuscript Received February 14, 2005

ABSTRACT: Using a series of A_nB_n miktoarm star block copolymers with different numbers of arms (n = 1, 2, 4, and 16), the effect of molecular architecture on the grain growth kinetics was investigated by annealing in supercritical carbon dioxide. Across this entire series of materials, all the A arms were polystyrene (PS) blocks from the same anionically synthesized batch, and all the B arms were polyisoprene (PI) blocks from the same anionically synthesized batch. Thus, all the star block copolymers employed in this study were composed of the same A and B arms linked together in symmetric numbers. The grain growth kinetics was monitored in real space by transmission electron microscopy (TEM), followed by subsequent micrograph image analysis. It was found that the molecular architecture influenced the grain growth kinetics of these A_nB_n star block copolymers significantly. The grain growth kinetics of these A_nB_n stars annealed in supercritical CO_2 was compared to a previously completed grain growth study of the same materials under simple thermal annealing. It was found that the grain growth kinetics for the A_nB_n stars with n = 2, 4, and 16 were similar for both supercritical CO_2 and thermal annealing. However, the grain growth kinetics of the diblock (A_nB_n with n = 1) was dramatically enhanced in supercritical CO_2 relative to thermal annealing.

Introduction

When block copolymer materials are brought from the disordered into ordered state, coherently ordered microdomain regions (i.e., grains) form with random orientations. Grain size and structure have been shown to be important for the mechanical and mass transport properties of block copolymers.[1−4] Block copolymers are also emerging as viable templates for nanostructured materials having applications in microelectronics. However, for applications requiring addressability, as in magnetic storage or as photonic materials, precise control of the grain size and structure is needed.[5,6]

The kinetics of grain growth of diblock copolymers, in the bulk, thin films, and solutions, have been studied by a variety of techniques, including small-angle X-ray scattering (SAXS),[7−9] transmission electron microscopy (TEM),[10,11] depolarized light scattering (DLS),[10,12−14] atomic force microscopy (AFM),[15] and polarized optical microscopy (POM).[16,17] As discussed by Gido and Thomas,[18] the long-range ordering of lamellar block copolymers has a dual nature. TEM images of these materials clearly show grain structures, similar to that of a metal, in which regions of coherent lamellar orientation are separated from one another by grain boundaries. This grain structure is generally accepted to be the result of nucleation and growth of grains analogous to grain growth in metals or ceramics.[19] Block copolymers with a lamellar morphology are materials with the same symmetry as smectic A liquid crystals. Their order is inherently soft and much more susceptible to structural distortions than inorganic materials. Thus, one frequently observes gentle changes in lamellar direction even within what might be classified as a single grain. Classical liquid crystalline defects, disclinations, are frequently observed in lamellar block copolymers in addition to the grain structure. The correlation functions and grain sizes obtained via image analysis in this study are clearly influenced by both types of orientational disorder, metal-like grains and liquid-crystal-like distortions. Thus, grain growth occurs by the motion of grain boundaries and other defects[20] and can be influenced by temperature (quench depth),[13,21,22] temperature gradient,[23] and molecular relaxation time.[21]

Prior research on grain growth kinetics in block copolymers has focused on diblock copolymers, and little is known about the effect of molecular architecture on grain growth kinetics. Recently, we have systematically investigated the effect of chain architecture on the grain growth kinetics of a series of A_nB_n star block copolymers,[24] where it was found that the star functionality strongly influenced the grain growth kinetics. However, the long annealing times required to achieve long-range order were limited by the thermal and/or oxidative stability of the copolymer.

It has been shown that supercritical CO_2 can be used to enhance the diffusion of small molecules in a glassy polymer matrix,[25,26] depress the glass transition temperatures of polymers,[27] and increase the mobility to enhance ordering of block copolymers.[28] Supercritical

* Corresponding authors: E-mail gido@mail.pse.umass.edu or russell@mail.pse.umass.edu.

10.1021/ma047774a CCC: $30.25
Published on Web 05/04/2005

Table 1. Molecular Characteristics of the A_nB_n Star Block Copolymers

sample	M_n[a] (g/mol)	M_w[b] (g/mol)	M_w/M_n[c]	wt % PS[d]
PS arm	19 000			100
PI arm	15 000			0
PS_1PI_1	36 200	36 300	1.05	55 ± 2
PS_2PI_2	64 000	66 000	1.04	56 ± 2
PS_4PI_4	121 000	127 500	1.04	54 ± 2
$PS_{16}PI_{16}$	*e*	533 000	1.07	59 ± 2

[a] Number-averaged molecular weight measured using membrane osmometry (MO) in toluene at 35 °C. [b] Weight-averaged molecular weight measured using low angle laser light scattering (LALLS) in THF at 25 °C. [c] Determined via size exclusion chromatography in THF at 25 °C (DRI detector). [d] Measured by ^{1}H NMR. [e] The molecular weight of this molecule is too high to be measured by MO.

CO_2 is a poor solvent for most polymers, and the equilibrium sorption of CO_2 is modest and can be tuned by temperature and pressure. RamachandraRao et al.[28] showed that supercritical CO_2 promoted the ordering of thin films of a deuterated, very high molecular weight poly(styrene-*b*-methyl methacrylate) diblock, producing an ordering that could not be achieved by thermal annealing.

Building upon these prior developments, the objective of the current work is to study the ordering kinetics of A_nB_n miktoarm star block copolymers annealed in supercritical CO_2. A series of A_nB_n miktoarm star copolymers (n = 1, 2, 4, and 16) were prepared using anionic living polymerization and a controlled chlorosilane coupling chemistry.[29] In these materials all the A arms are polystyrene (PS) blocks from the same ionic polymerization batch and are, thus, characteristically the same. Likewise, all the B arms are polyisoprene (PI) blocks from the same ionic polymerization batch and are, thus, characteristically the same. This enables us to exclude any variables from the study that would arise from differences in the composition of the constituent arms.

Experimental Section

The A_nB_n star block copolymers used in this study were prepared by living anionic polymerization of styrene and isoprene followed by a controlled chlorosilane coupling chemistry and purification. Table 1 shows their molecular characteristics. On the basis of the composition of these A_nB_n stars, a lamellar morphology is expected and confirmed experimentally by SAXS and TEM for all these stars. The detailed synthesis, molecular characterization, and basic morphologies of these star copolymers have been described elsewhere.[29]

Sample Preparation. Five weight percent solutions of each of the four star copolymers were prepared in toluene, a neutral solvent for the PS and PI blocks. Bulk films, about 1 mm thick, were obtained by evaporating the solvent from these solutions. Previous studies on the PS- and PI-based block copolymer morphology involved slow solvent evaporation, which usually takes place over 1 or 2 weeks.[29−33] Slow solvent removal enhances the grain size and long-range order even prior to thermal annealing. In the present study, an initial microphase-separated morphology with numerous small grains is desired as a starting point for the observation of grain growth. To produce small grains, the samples were cast very rapidly and were dried for 2 days at room temperature under vacuum. These dried films constituted the starting point (time t = 0) for the grain growth studies.

The dried polymer films were then annealed at 80 °C in supercritical CO_2 at a pressure of 172 bar, using an ISCO high-pressure syringe pump, for different periods of time. A controlled depressurization was performed to avoid foaming of the sample. All samples were cast and annealed together to ensure identical external conditions. Pieces of films for each sample were removed from the high-pressure vessel at different times, from 1 day up to 16 days, and the grain size was characterized.

TEM Characterization. All samples for transmission electron microscopy (TEM) were microtomed using a Leica Ultracut UCT cryoultramicrotome. Thin sections 50−100 nm in thickness were cut with a Diatome diamond knife at −100 °C. To reduce sampling bias in the collection of TEM micrographs, several different parts of each sample were microtomed. These sections were then collected on 400 mesh copper TEM grids and stained in OsO_4 vapor for 6 h. TEM was performed on a JEOL 2000 FX instrument, operated at accelerating voltages of 200 kV. TEM magnifications were calibrated with an etched silica standard. Relatively low magnification, 8000×, was used for all the micrographs to ensure that each micrograph encompassed as many complete grains as possible for the subsequent statistical analysis. Fifty TEM micrographs per sample per annealing time were used for the quantitative image analysis of grain size.

Quantitative Image Analysis. Grain size is obtained using the methods developed by Garetz, Balsara, and coworkers.[10,11,34] Details can be found in previous studies on the grain growth kinetics.[24] In general, local Fourier transform (LFT) is performed to determine the local orientation of lamellar normal, $\phi(\mathbf{r})$. Based on orientations of lamellar normal, two correlation functions, $C(\mathbf{r})_{\|}$ and $C(\mathbf{r})_{\perp}$, are generated to account for the anisotropy of grain shape:[10]

$$C(|\mathbf{r}'-\mathbf{r}''|) \approx \langle \cos\{2[\phi(\mathbf{r}') - \phi(\mathbf{r}'')]\}\rangle$$

where $C(r)_{\|}$ represents the correlation function in the direction of lamellar normal and $C(r)_{\perp}$ is the correlation function in the direction perpendicular to lamellar normal. From these two correlation functions the corresponding correlation lengths can be extracted. One is in the direction of the lamellar normal, denoted as $\kappa_{\|}$, and the other one is perpendicular to lamellar normal, denoted as $\kappa_{\perp}$. Both $\kappa_{\|}$ and $\kappa_{\perp}$ are used to characterize grain size.

Results and Discussion

Figure 1a shows a TEM micrograph of the unannealed A_4B_4 sample, i.e., t = 0, that is microphase separated into a lamellar morphology as a result of the solution casting, but the grain size is quite small. Figure 1b,c shows TEM images of the same A_4B_4 sample after thermal annealing at 120 °C for 60 days and after annealing in supercritical CO_2 at 172 bar and 80 °C for 8 days. It is clear that both annealing methods produce a significant increase in grain size.

Figure 2 shows both correlation functions, $C(r)_{\|}$ and $C(r)_{\perp}$, for the $A_{16}B_{16}$ copolymer. Each curve was fit to an exponential function of the form $\exp(-r/\kappa)$, as shown in the inset, where κ is the correlation length, a characteristic dimension of the grain structure. The grains are generally anisotropic in shape, being larger parallel to the lamellar normal and smaller perpendicular to the lamellar normal, which is consistent with previous studies.[10,20,35,36] Consequently, both correlation lengths are used to characterize grain growth. The correlation length in the direction of lamellar normal is denoted as $\kappa_{\|}$, and the correlation length perpendicular to the lamellar normal is denoted as $\kappa_{\perp}$.

Table 2 and Figure 3a−d show the time evolution of the characteristic grain size for the A_nB_n series of materials when annealed in supercritical CO_2 at 172 bar and 80 °C. The anisotropic grain shape is evidenced by the fact that $\kappa_{\|} > \kappa_{\perp}$ for all the copolymers across the full range of annealing times. Least-squares fits of power law functions of the form $\kappa = At^{\nu}$ are shown as dash and dash−dotted lines. The A and ν parameters

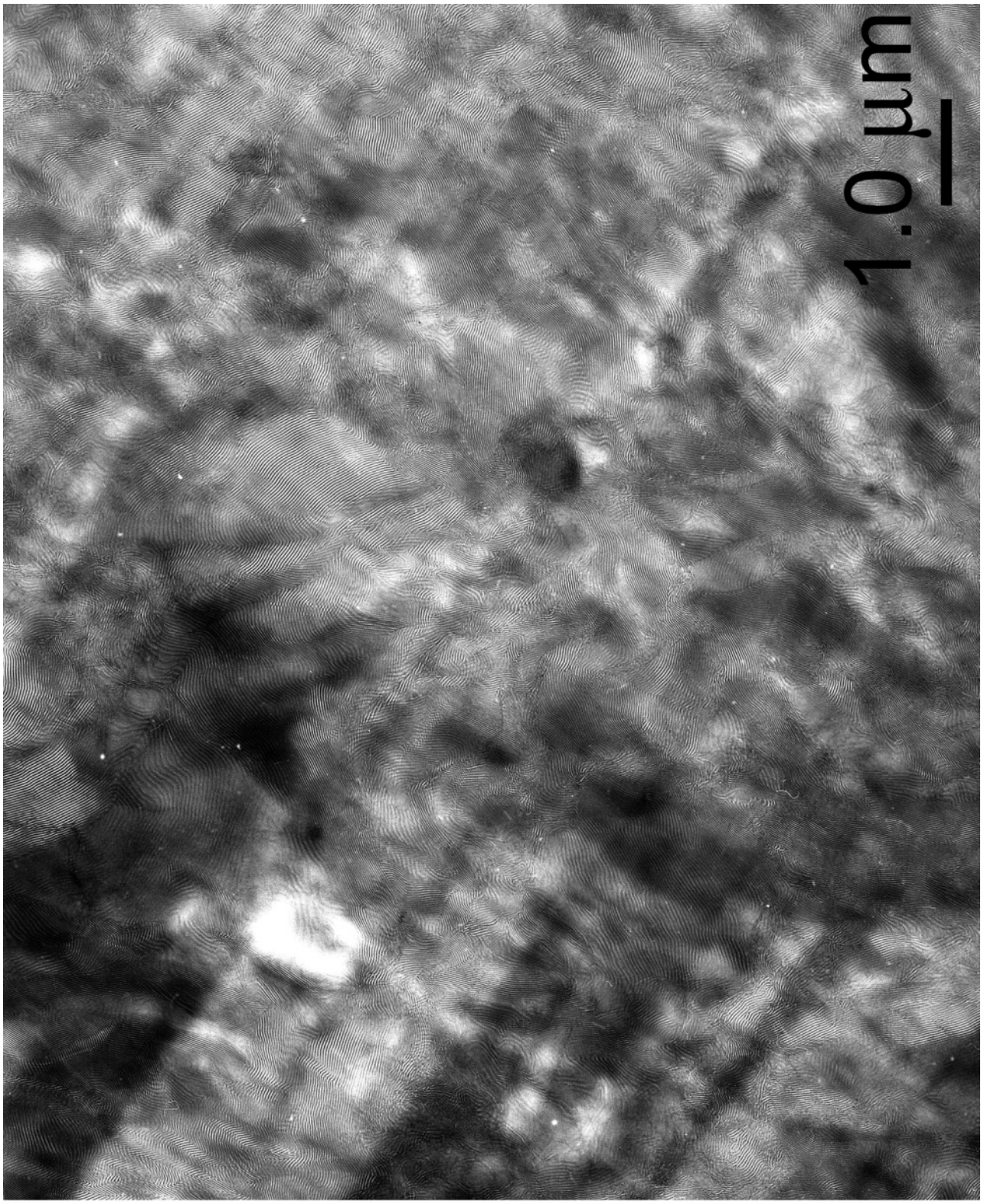

(a)

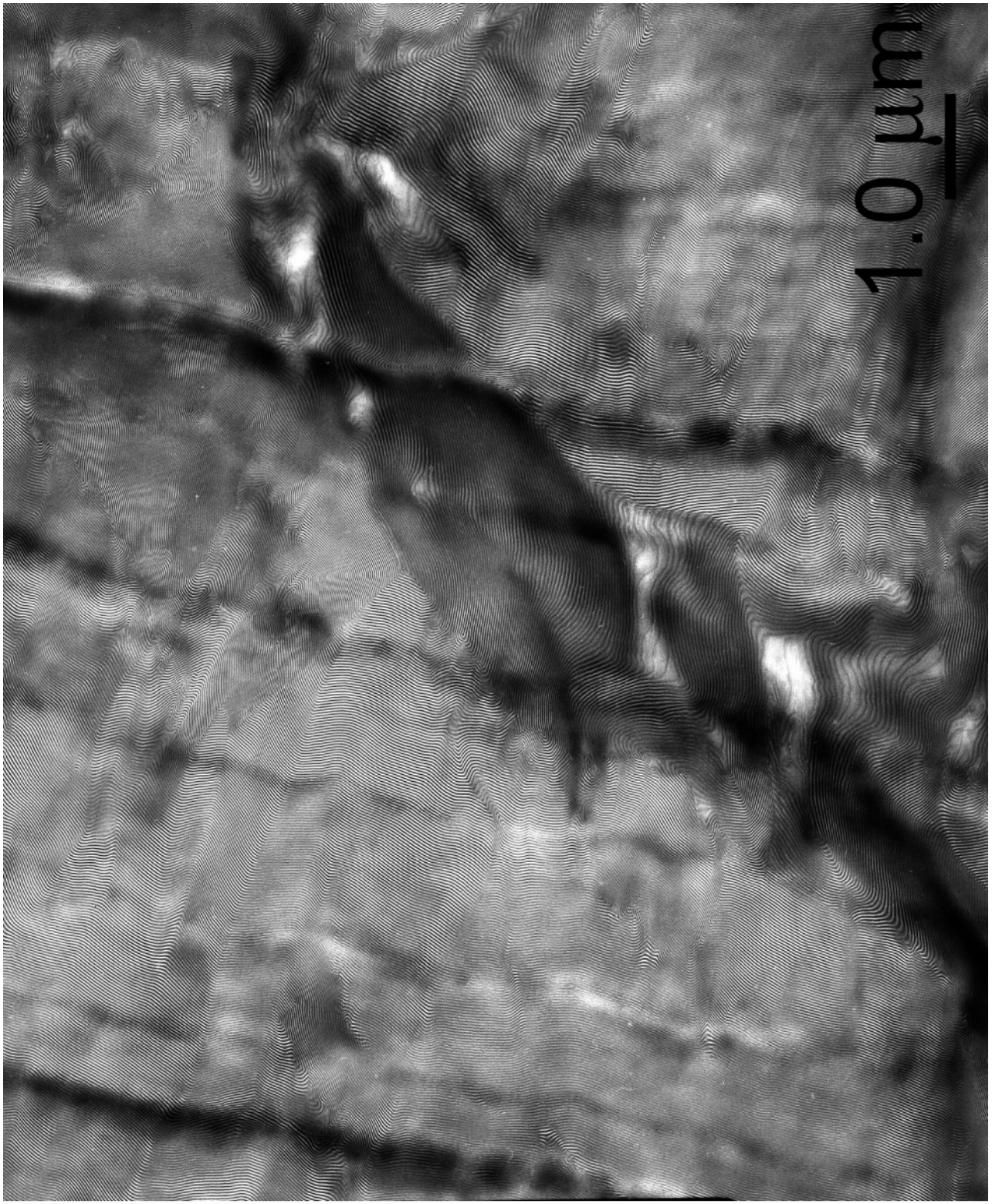

(g)

Figure 1. Representative TEM images of A_4B_4 star block copolymer: (a) immediately after solution casting, i.e., $t = 0$; (b) after thermal annealing for 60 days at 120 °C; and (c) after annealing in supercritical CO_2 for 8 days at 172 bar and 80 °C.

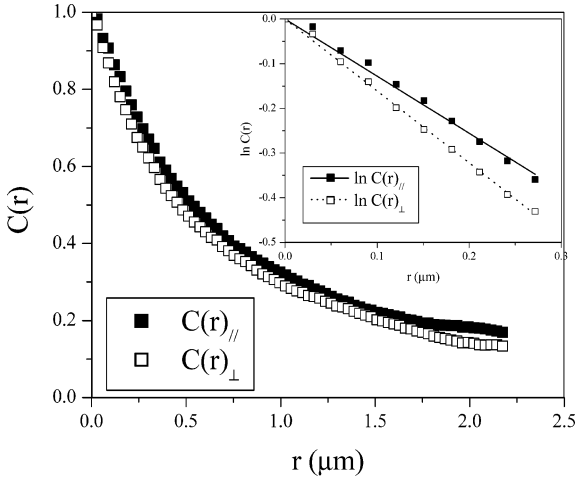

Figure 2. Correlation functions for $A_{16}B_{16}$ star block copolymer parallel ($C_{||}$) and perpendicular ($C_{\perp}$) to the lamellar normal after annealing in supercritical CO_2 at 172 bar and 80 °C for 96 h. Inset: logarithmic scale with least-squares exponential fit of the first 10 points of each correlation function.

determined are given on the left-hand side of Table 3. To within experimental errors, the $\kappa_{||}$ and $\kappa_{\perp}$ fits, on the log−log scale in Figure 3a−d, are parallel for each material, indicating that the grain anisotropy does not change significantly during grain structure coarsening.

The grain volume, estimated as $(\kappa_{||}) \times (\kappa_{\perp}) \times (\kappa_{\perp})$, is shown in Figure 4a as a function of annealing time for all the A_nB_n samples. On the basis of previous work of Balsara and co-workers,[20] it is expected that the time evolution of average grain volume (V) obeys a power law: $V \sim t^{\beta}$. They reported β for both pre- and post-impingement grain growth in a cylinder forming diblock copolymer of low molecular weight. Their post-impingement β value of 1.20 is more relevant than the pre-impingement value for comparison to our current results. However, Balsara's work was on cylinder grain growth and ours is on lamellar. This may contribute to differences in the observed growth exponents. Harrison et al.[15] have investigated the ordering kinetics in thin films of a cylindrical diblock copolymer and found that the correlation length, κ, increased with annealing time as $\sim t^{1/4}$.

Shown in Figure 4a are log−log plots of V vs t. The exponent, β, and prefactor, A, for each architecture are given on the left-hand side of Table 4. As can be seen, β for all the star architectures is similar, ranging from 0.35 to 0.37. However, β for the diblock A_1B_1 is quite different, ∼0.80. Thus, the simple diblock copolymer grains coarsen much more rapidly than the other architectures, which is significantly different from the results obtained by thermal annealing.[24]

Figure 3a−d also shows the comparison of the increase in $\kappa_{||}$ and $\kappa_{\perp}$, with annealing time for the A_nB_n stars. Each curve compares grain growth under thermal annealing at 120 °C to annealing of the same material in supercritical CO_2 at 172 bar and 80 °C. As for grain growth kinetics, Kramer et al. have shown that it is necessary to balance the ordering kinetics with the thermodynamic driving force for microphase separation of block copolymers in order to obtain a high degree of order.[37] Similar results have also been reported by Balsara and co-workers on the grain growth rates in a polystyrene-*b*-polyisoprene diblock copolymer melt.[14] However, the thermal mobility, proportional to $(T - T_g)$ where T_g is the glass transition temperature, and the thermodynamic driving force, proportional to $(T_{ODT} - T)$ where T_{ODT} is the order-to-disorder transition temperature, exhibit opposite dependence on temperatures. As a result, an optimum annealing temperature exists due to the interplay between these two opposite dependences.

Using the Sanchez−Lacombe equation of state,[38] the weight fraction of CO_2 dissolved in the PS block of these A_nB_n star block copolymers is estimated to be about 8.5% under the current conditions, with characteristic parameters for CO_2 and PS taken from the literature.[39,40] Sorption data of CO_2 in PS at 80 °C are not available. Therefore, following the approach of Watkins and co-workers,[41] the interaction parameter determined at 35 °C is used for our calculations. The order-to-disorder transition temperature (T_{ODT}) of pure A_1B_1 is measured to be 293 °C, and that of pure $A_{16}B_{16}$ is 420 °C.[42] Following the method of Lodge and co-workers[43] and assuming that CO_2 is uniformly distributed in these A_nB_n star block copolymers (CO_2 is slightly selective for polyisoprene[41]), the thermodynamic driving force ($T_{ODT} - T$) for the A_1B_1 diblock copolymer is calculated to be about 170 °C for both thermal annealing and supercritical CO_2 annealing in our study. Similarly, the ($T_{ODT} - T$) for the $A_{16}B_{16}$ star block copolymer is estimated to

Table 2. Correlation Lengths of A_nB_n Star Block Copolymers during Annealing in Supercritical CO_2 at 172 bar and 80 °C As Determined by TEM and Image Analysis[a]

	PS_1PI_1				PS_2PI_2			
time (h)	$\kappa_{||}$ (μm)	$\sigma_{||}$ (μm)	$\kappa_{\perp}$ (μm)	$\sigma_{\perp}$ (μm)	$\kappa_{||}$ (μm)	$\sigma_{||}$ (μm)	$\kappa_{\perp}$ (μm)	$\sigma_{\perp}$ (μm)
0	0.26	0.03	0.22	0.02	0.74	0.02	0.47	0.01
24	0.33	0.01	0.32	0.02	0.81	0.01	0.53	0.02
48	0.53	0.01	0.44	0.01	0.82	0.02	0.67	0.02
96	0.73	0.02	0.49	0.03	0.94	0.04	0.74	0.02
192	0.85	0.08	0.60	0.05	0.96	0.04	0.75	0.02
384	0.91	0.04	0.60	0.03	0.96	0.04	0.82	0.03
	PS_4PI_4				$PS_{16}PI_{16}$			
time (h)	$\kappa_{||}$ (μm)	$\sigma_{||}$ (μm)	$\kappa_{\perp}$ (μm)	$\sigma_{\perp}$ (μm)	$\kappa_{||}$ (μm)	$\sigma_{||}$ (μm)	$\kappa_{\perp}$ (μm)	$\sigma_{\perp}$ (μm)
0	0.29	0.02	0.30	0.02	0.57	0.01	0.50	0.02
24	1.00	0.02	0.73	0.01	0.61	0.02	0.51	0.01
48	1.18	0.02	0.86	0.04	0.72	0.02	0.53	0.01
96	1.33	0.03	0.95	0.03	0.78	0.03	0.62	0.01
192	1.43	0.03	0.98	0.03	0.85	0.02	0.63	0.02
384	1.43	0.06	1.02	0.02	0.86	0.07	0.69	0.05

[a] Correlation lengths parallel and perpendicular ($\kappa_{||}$ and $\kappa_{\perp}$) to the lamellar normal and the standard deviations of $\kappa_{||}$ and $\kappa_{\perp}$ ($\sigma_{||}$ and $\sigma_{\perp}$) are tabulated.

Table 3. Comparisons of Power Law Fitting Parameters for Correlation Length Growth Data of the A_nB_n Star Block Copolymers between Thermal Annealing at 120 °C and Annealing in Supercritical CO_2 at 172 bar and 80 °C: $\kappa = At^{\nu}$

	supercritical CO_2 annealing				thermal annealing			
sample	$A_{\|}$	$A_{\perp}$	$\nu_{\|}$	$\nu_{\perp}$	$A_{\|}$	$A_{\perp}$	$\nu_{\|}$	$\nu_{\perp}$
PS_1PI_1	0.12	0.17	0.36	0.23	0.86	0.68	0.07	0.06
PS_2PI_2	0.65	0.35	0.07	0.15	1.00	0.66	0.10	0.13
PS_4PI_4	0.69	0.53	0.13	0.12	0.59	0.49	0.14	0.13
$PS_{16}PI_{16}$	0.44	0.35	0.12	0.11	0.44	0.37	0.10	0.13

be about 300 °C under both thermal and supercritical CO_2 annealing conditions. Therefore, the thermodynamic driving force for each individual A_nB_n star under thermal annealing is about the same as that in supercritical CO_2 annealing, which allows comparison of its grain growth kinetics under these two different annealing methods. While it is therefore possible to compare grain growth under thermal and supercritical CO_2 annealing for each A_nB_n sample individually, it is not possible to choose annealing conditions that keeps the thermodynamic driving force constant across the entire A_nB_n series.

Table 3 summarizes the results of power law fitting to the growth of the two correlation lengths, with results for supercritical CO_2 on the left-hand side and results for thermal annealing on the right-hand side. For these A_nB_n stars, the glass transition temperature (T_g) of the PS block in these materials is determined to be about 85 °C. Based on the Chow model,[44] the T_g of the PS block in these materials, under the current supercritical CO_2 annealing condition, is calculated to be ~20 °C with system-dependent constants taken from the literature.[45] Thus, $(T - T_g)$ of these A_nB_n star block copolymers in supercritical CO_2 annealing is about 60 °C. On the other hand, for the simple thermal annealing case, the corresponding $(T - T_g)$ is ~35 °C. Therefore, supercritical CO_2 has enhanced the mobility of these A_nB_n star materials at a temperature (80 °C) lower than the thermal annealing temperature (120 °C) while keeping the thermodynamic driving force for ordering constant.

Within the experimental error, however, the growth rate in supercritical CO_2 is the same as that under thermal annealing for the A_nB_n stars where $n = 2$, 4, and 16. However, for the A_1B_1 diblock, the grain growth rate is much faster with supercritical CO_2 than thermal annealing. This difference in grain growth kinetics for the diblock under different annealing conditions is even more evident when the corresponding grain volumes are plotted for thermal annealing and for supercritical CO_2 annealing in Figure 4a,b. For the A_nB_n stars where $n = 2$, 4, and 16, regardless of annealing method, the grains grow at about the same rate as shown in Figure 4a,b. However, for the A_1B_1 diblock, the grains are found to grow much more rapidly in supercritical CO_2 than by thermal annealing.

Our grain growth data suggest a fundamental difference in the mechanisms of grain growth in the A_1B_1 diblock versus all of the A_nB_n stars (for $n = 2$, 4, and 16) under both thermal and supercritical CO_2 annealing. While the mechanism of grain growth appears to be similar for all the stars under both annealing conditions, the diblock material seems different. Two mechanisms have been proposed for diffusion of diblock copolymers in the lamellar plane, while the diffusion perpendicular to the lamellar planes is dictated by a thermodynamic barrier determined by the combination of temperature and molecular weight.[46] At low degrees of segregation ($\chi N < 20$), the diffusion in the lamellar planes occurs by an activated reptation mechanism, while at higher degrees of segregation ($\chi N > 20$) a block retraction mechanism is thought to occur.[46]

We previously hypothesized that the difference between the A_1B_1 diblock and the various A_nB_n ($n = 2$, 4, and 16) stars is related to molecular entanglements. As illustrated in Figure 5, tilt grain boundaries cannot move by molecular motions along the interface alone. Some interfacial breaking and re-forming (i.e., diffusion of chains normal to the lamellar layers) is necessary to move this type of grain boundary. Figure 5 illustrates that in order to move the chevron grain boundary to the right lamellar layers indicated by an "×" must break and then re-form to change the partnering of layers on either side of the boundary. It may, however, be possible for twist grain boundaries with Scherk saddle surface interfaces[18,47] to move through the sample via a mechanism in which the interfaces remain intact; i.e., only diffusion along existing interfaces is required.

The molecular weight of the A_1B_1 diblock is such that it is slightly entangled. Previous work by Zhu et al.[29] has shown that, in the microphase-separated state, the A_nB_n stars for $n = 2$, 4, and 16 are between 5 and 12% more stretched normal to the interface than the corresponding A_1B_1 diblock due to the effect of arm crowding near the $2n$ functional junction point. This additional chain stretching normal to the interface reduces entanglements with neighboring copolymers, thereby increasing the rate at which the A_nB_n ($n = 2$, 4, and 16) stars can diffuse within the lamellar layers relative to the corresponding diblock. Lodge and co-workers have shown that the diffusion of entangled block copolymers is significantly retarded due to a combination of the degree of microphase segregation and entanglement constraints.[46,48] For the entangled A_1B_1 diblock, under the thermal annealing condition studied here, χN is calculated to be about 30. Thus, diffusion of a single chain in the lamellar plane would occur, most likely, by the block retraction mechanism, where a block retracts via reptation through the entanglement constraints into the interfacial zone and then reextends into a new conformation.

However, by annealing in supercritical CO_2, the volume dilation of the material with CO_2 can reduce entanglements, even in the A_1B_1 diblock. Therefore, the block-retraction mechanism of chain diffusion may not be necessary in the supercritical CO_2 case. In addition, it has been shown that supercritical CO_2 can depress the upper order−disorder transition (UODT) of a styrene−isoprene diblock copolymer by as much as 45 °C.[41] Thus, the screening effect of supercritical CO_2 on unfavorable interactions between the dissimilar segments may also facilitate the diffusion of polymer chains in a microphase-separated state by reducing the thermodynamic barrier (effective χN) to diffusion perpendicular to the lamellar layers. This type of diffusion is necessary to facilitate motion of chevron tilt grain boundaries during grain growth. To the extent that

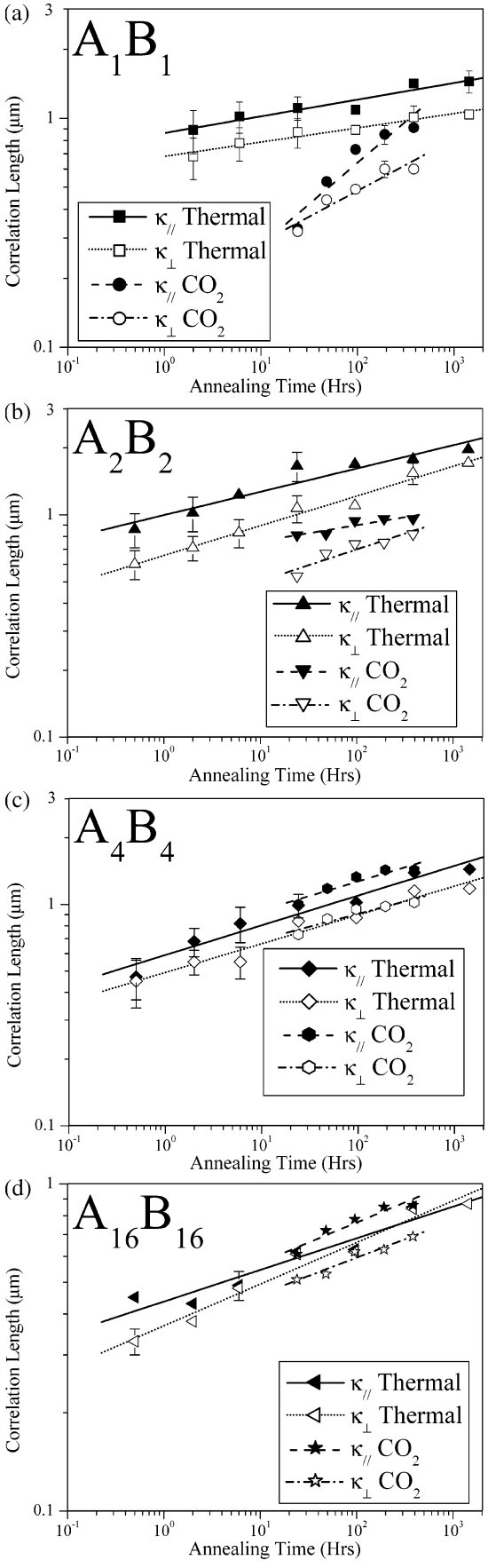

Figure 3. Comparison of the growth of correlation lengths in the A_nB_n star block copolymers between supercritical CO_2 annealing and thermal annealing: (a) A_1B_1, (b) A_2B_2, (c) A_4B_4, and (d) $A_{16}B_{16}$. The lines in each plot are the least-squares, power law fits to the corresponding correlation length.

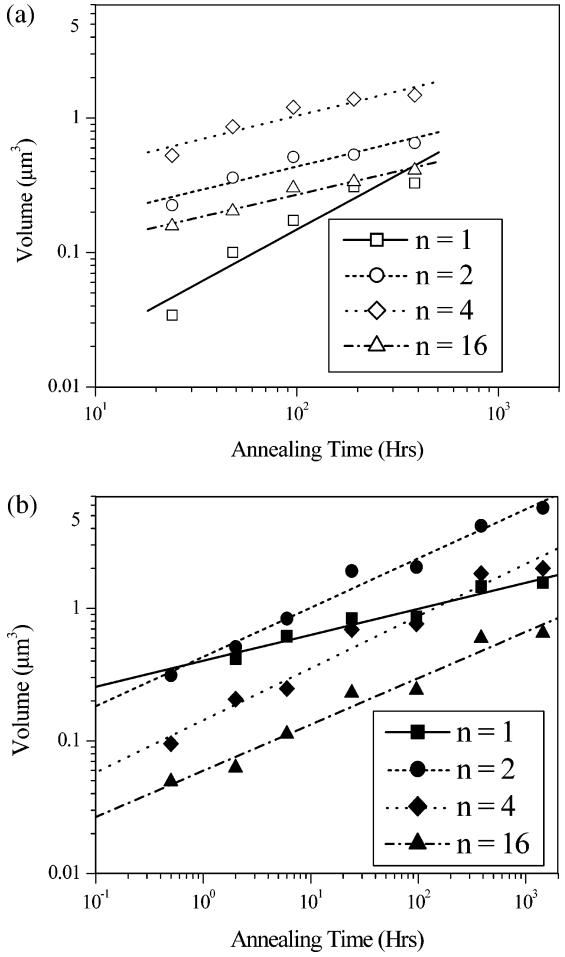

Figure 4. Effect of arm number, n, on the growth of grain volumes in the A_nB_n star block copolymers under (a) supercritical CO_2 annealing and (b) thermal annealing. The lines in the plot are the least-squares, power law fits to the corresponding grain volume data.

Table 4. Comparisons of Power Law Fitting Parameters for Grain Volume Growth Data of the A_nB_n Star Block Copolymers between Thermal Annealing at 120 °C and Annealing in Supercritical CO_2 at 172 bar and 80 °C: $V = A_v t^{\beta}$

	supercritical CO_2 annealing		thermal annealing	
sample	A_v	β	A_v	β
PS_1PI_1	0.003	0.82 ± 0.14	0.40	0.20 ± 0.02
PS_2PI_2	0.08	0.36 ± 0.07	0.43	0.37 ± 0.02
PS_4PI_4	0.19	0.37 ± 0.07	0.14	0.39 ± 0.03
$PS_{16}PI_{16}$	0.05	0.35 ± 0.04	0.06	0.35 ± 0.03

chevron grain boundaries represent a large population of the grain boundaries in a sample, the enhancement of their mobility in supercritical CO_2 may contribute to the significant increase in grain growth rate observed in the diblock.

Thus, we can postulate that for the A_nB_n (n = 2, 4, and 16) stars in supercritical CO_2 the enhancement of diffusion normal to the lamellar layers is not as pronounced as in the diblock case, since the thermodynamic barrier ($n\chi N$) is higher due to the presence of multiple arms which need to be pulled across a domain of the opposing material. For these stars, there is little entanglement hindrance to diffusion parallel to the lamellar layers under both thermal and supercritical CO_2 annealing, hence the similarity of growth rate for the stars under both types of annealing.

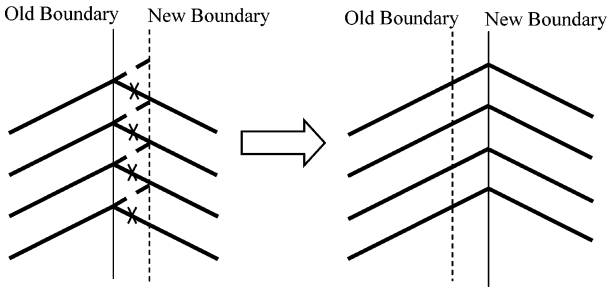

Figure 5. Schematic motion of a chevron tilt grain boundary. If the lamellar orientation on both sides of the boundary is to be preserved, then the motion must involve breaking and reforming of interfaces as indicated by ×'s and dashed lines in the diagram.

Conclusions

Supercritical CO_2 can be used to promote the grain growth of all these A_nB_n ($n = 1$, 2, 4, and 16) star block copolymers at relatively low temperatures. Their grain growth kinetics in supercritical CO_2 shows a different dependence on the number of arms, n, than that of the same series when thermally annealed. Grains of the A_1B_1 diblock are found to grow faster in supercritical CO_2 than in the thermal annealing case. Supercritical CO_2 did not change the grain growth kinetics of the A_nB_n ($n = 2$, 4, and 16) stars, however, under the conditions studied here. Their grain growth kinetics in supercritical CO_2 is found to be the same as that in the thermal annealing case. Comparison of the scaling relationships suggests that the difference in the grain growth kinetics between the A_1B_1 diblock and the various A_nB_n ($n = 2$, 4, and 16) stars can be attributed to differences in molecular entanglements and to the thermodynamic barrier to diffusion perpendicular to the lamellar layers.

Acknowledgment. We acknowledge support from the U.S. Army Research Laboratory−Polymer Materials Center of Excellence, the central facilities of the NSF-supported Material Research Science and Engineering Center (MRSEC) at the University of Massachusetts—Amherst, and the W.M. Keck Electron Microscopy Laboratory. B.G. and F.A. gratefully acknowledge financial support provided by the National Science Foundation, Grant DMR-0213508. The assistance of Sievert and Lavery with the supercritical CO_2 experimental setup is also acknowledged.

References and Notes

(1) Kawasaki, K.; Onuki, A. *Phys. Rev. A* **1990**, *42*, 3664−3666.
(2) Csernica, J.; Baddour, R. F.; Cohen, R. E. *Macromolecules* **1989**, *22*, 1493−1496.
(3) Rein, D. H.; Csernica, J.; Baddour, R. F.; Cohen, R. E. *Macromolecules* **1990**, *23*, 4456−4460.
(4) Csernica, J.; Baddour, R. F.; Cohen, R. E. *Macromolecules* **1990**, *23*, 1429−1433.
(5) Park, M.; Harrison, C.; Chaikin, P. M.; Register, R. A.; Adamson, D. H. *Science* **1997**, *276*, 1401−1404.
(6) Li, R. R.; Dapkus, P. D.; Thompson, M. E.; Jeong, W. G.; Harrison, C.; Chaikin, P. M.; Register, R. A.; Adamson, D. H. *Appl. Phys. Lett.* **2000**, *76*, 1689−1691.
(7) Harkless, C. R.; Singh, M. A.; Nagler, S. E.; Stephenson, G. B.; Jordansweet, J. L. *Phys. Rev. Lett.* **1990**, *64*, 2285−2288.
(8) Singh, M. A.; Harkless, C. R.; Nagler, S. E.; Shannon, R. F.; Ghosh, S. S. *Phys. Rev. B* **1993**, *47*, 8425−8435.
(9) Myers, R. T.; Cohen, R. E.; Bellare, A. *Macromolecules* **1999**, *32*, 2706−2711.
(10) Chang, M. Y.; Abuzaina, F. M.; Kim, W. G.; Gupton, J. P.; Garetz, B. A.; Newstein, M. C.; Balsara, N. P.; Yang, L.; Gido, S. P.; Cohen, R. E.; Boontongkong, Y.; Bellare, A. *Macromolecules* **2002**, *35*, 4437−4447.
(11) Beyer, F. L.; Gido, S. P.; Buschl, C.; Iatrou, H.; Uhrig, D.; Mays, J. W.; Chang, M. Y.; Garetz, B. A.; Balsara, N. P.; Beck Tan, N.; Hadjichristidis, N. *Macromolecules* **2000**, *33*, 2039−2048.
(12) Wang, H.; Newstein, M. C.; Chang, M. Y.; Balsara, N. P.; Garetz, B. A. *Macromolecules* **2000**, *33*, 3719−3730.
(13) Newstein, M. C.; Garetz, B. A.; Balsara, N. P.; Chang, M. Y.; Dai, H. J. *Macromolecules* **1998**, *31*, 64−76.
(14) Kim, W. G.; Garetz, B. A.; Newstein, M. C.; Balsara, N. P. *J. Polym. Sci., Part B: Polym. Phys.* **2001**, *39*, 2231−2242.
(15) Harrison, C.; Adamson, D. H.; Cheng, Z. D.; Sebastian, J. M.; Sethuraman, S.; Huse, D. A.; Register, R. A.; Chaikin, P. M. *Science* **2000**, *290*, 1558−1560.
(16) Chastek, T. Q.; Lodge, T. P. *Macromolecules* **2003**, *36*, 7672−7680.
(17) Chastek, T. Q.; Lodge, T. P. *Macromolecules* **2004**, *37*, 4891−4899.
(18) Gido, S. P.; Thomas, E. L. *Macromolecules* **1994**, *27*, 849−861.
(19) Fredrickson, G. H.; Binder, K. *J. Chem. Phys.* **1989**, *91*, 7265−7275.
(20) Dai, H. J.; Balsara, N. P.; Garetz, B. A.; Newstein, M. C. *Phys. Rev. Lett.* **1996**, *77*, 3677−3680.
(21) Balsara, N. P.; Garetz, B. A.; Chang, M. Y.; Dal, H. J.; Newstein, M. C. *Macromolecules* **1998**, *31*, 5309−5315.
(22) Kim, W. G.; Chang, M. Y.; Garetz, B. A.; Newstein, M. C.; Balsara, N. P.; Lee, J. H.; Hahn, H.; Patel, S. S. *J. Chem. Phys.* **2001**, *114*, 10196−10211.
(23) Bodycomb, J.; Funaki, Y.; Kimishima, K.; Hashimoto, T. *Macromolecules* **1999**, *32*, 2075−2077.
(24) Hu, X. C.; Zhu, Y. Q.; Gido, S. P.; Russell, T. P.; Iatrou, H.; Hadjichristidis, N.; Abuzaina, F. M.; Garetz, B. A. *Faraday Discuss.* **2005**, *128*, 103−112.
(25) Chapman, B. R.; Gochanour, C. R.; Paulaitis, M. E. *Macromolecules* **1996**, *29*, 5635−5649.
(26) Berens, A. R.; Huvard, G. S.; Korsmeyer, R. W.; Kunig, F. W. *J. Appl. Polym. Sci.* **1992**, *46*, 231−242.
(27) Condo, P. D.; Johnston, K. P. *J. Polym. Sci., Part B: Polym. Phys.* **1994**, *32*, 523−533.
(28) RamachandraRao, V. S.; Gupta, R. R.; Russell, T. P.; Watkins, J. J. *Macromolecules* **2001**, *34*, 7923−7925.
(29) Zhu, Y. Q.; Gido, S. P.; Moshakou, M.; Iatrou, H.; Hadjichristidis, N.; Park, S.; Chang, T. *Macromolecules* **2003**, *36*, 5719−5724.
(30) Zhu, Y. Q.; Weidisch, R.; Gido, S. P.; Velis, G.; Hadjichristidis, N. *Macromolecules* **2002**, *35*, 5903−5909.
(31) Beyer, F. L.; Gido, S. P.; Uhrig, D.; Mays, J. W.; Beck Tan, N.; Trevino, S. F. *J. Polym. Sci., Part B: Polym. Phys.* **1999**, *37*, 3392−3400.
(32) Beyer, F. L.; Gido, S. P.; Poulos, Y.; Avgeropoulos, A.; Hadjichristidis, N. *Macromolecules* **1997**, *30*, 2373−2376.
(33) Beyer, F. L.; Gido, S. P.; Velis, G.; Hadjichristidis, N.; Beck Tan, N. *Macromolecules* **1999**, *32*, 6604−6607.
(34) Garetz, B. A.; Balsara, N. P.; Dai, H. J.; Wang, Z.; Newstein, M. C.; Majumdar, B. *Macromolecules* **1996**, *29*, 4675−4679.
(35) Balsara, N. P.; Marques, C. M.; Garetz, B. A.; Newstein, M. C.; Gido, S. P. *Phys. Rev. E* **2002**, *66*.
(36) Hashimoto, T.; Sakamoto, N. *Macromolecules* **1995**, *28*, 4779−4781.
(37) Segalman, R. A.; Hexemer, A.; Hayward, R. C.; Kramer, E. J. *Macromolecules* **2003**, *36*, 3272−3288.
(38) Sanchez, I. C.; Lacombe, R. H. *Macromolecules* **1978**, *11*, 1145−1156.
(39) Kiszka, M. B.; Meilchen, M. A.; McHugh, M. A. *J. Appl. Polym. Sci.* **1988**, *36*, 583−597.
(40) Lemmon, E. W.; McLinden, M. O.; Friend, D. G. Thermophysical Properties of Fluid Systems. In *NIST Chemistry WebBook, NIST Standard Reference Database No. 69*; Mallard, W. G., Linstrom, P. J., Eds.; National Institute of Standards and Technology: Gaithersburg, MD; Nov 1998.
(41) Vogt, B. D.; Brown, G. D.; RamachandraRao, V. S.; Watkins, J. J. *Macromolecules* **1999**, *32*, 7907−7912.
(42) Hu, X.; Gomez, E. D.; Balsara, N. P.; Iatrou, H.; Hadjichristidis, N.; Gido, S. P.; Russell, T. P., unpublished results.
(43) Lodge, T. P.; Hanley, K. J.; Pudil, B.; Alahapperuma, V. *Macromolecules* **2003**, *36*, 816−822.
(44) Chow, T. S. *Macromolecules* **1980**, *13*, 362−364.
(45) Gupta, R. R.; Lavery, K. A.; Francis, T. J.; Webster, J. R. P.; Smith, G. S.; Russell, T. P.; Watkins, J. J. *Macromolecules* **2003**, *36*, 346−352.

(46) Lodge, T. P.; Dalvi, M. C. *Phys. Rev. Lett.* **1995**, *75*, 657−660.
(47) Gido, S. P.; Gunther, J.; Thomas, E. L.; Hoffman, D. *Macromolecules* **1993**, *26*, 4506−4520.
(48) Dalvi, M. C.; Eastman, C. E.; Lodge, T. P. *Phys. Rev. Lett.* **1993**, *71*, 2591−2594.

MA047774A